The Ciência & Engenharia - Science & Engineering Journal
ISSN: 0103-944X
Volume 11 Issue 1, 2023
pp: 122 - 131

Hardened Enhancement Investigation of Al-Zr-N Coating by EBM Technique: A review

R Hariharan[1], Pati Lacha Gopal[2], A Abhishek[3], P Selva Raj[4], G Ashok Kumar[5] , V Balambica[6]

[1,6]Department of Mechanical Engineering, Bharath Institute of Higher Education and Research, Chennai-73, Tamilnadu, India

[2,3,4,5]Students, Department of Mechanical Engineering, Bharath Institute of Higher Education and Research, Chennai-73, Tamilnadu, India

Abstract

The purpose of this research is to examine the Al-Zr-N coating applied to the E19 steel alloy by physical vapour deposition using an electron beam. The physical vapour deposition processes used to create layered [Al-Zr-N] coatings and the structures, wear resistances, and corrosion behaviours of these materials. In order to examine the coating structures, surface roughness, micro-hardness, micro-abrasion, and pin on disc were used. One of the residual stress elements that can lead to failure mechanisms for suitable coatings is thermal stress. The mechanical characteristics of the coating, including its deposition temperature, young's modulus, thermal expansion coefficient, and substrate and coating thickness, were investigated using a validated computational simulation in this paper.

Keywords: E19 steel, residual stress, Al-Zr-N, electron beam physical vapour deposition

1. Introduction

As protective coatings for corrosion and wear resistance, thin hard coatings of transitional metal nitrides created by electron beam physical vapour deposition are now extensively used. First and foremost, it's because they have better mechanical qualities like increased hardness, strong oxidation and corrosion resistance, and wear resistance. Nanostructured materials can be created by changing various the alternate depositions of two materials to form a multilayer thin sheet, which has several significant advantages.

Due to their superior mechanical and tribological qualities, thin hard coverings are frequently used on industrial components. The coating's hardness works to the substrate's benefit by reducing abrasive wear [1]. The ZrN coating is one of the thin coatings that are best at offering high abrasion protection, low friction, and high hardness [2]. Various base materials, including aluminium and its alloys, have had their service lives extended using the ZrN coating. The corrosion, hardness, and wear resilience of the substrate materials had been enhanced, according to [3], by using ZrN coating. ZrN coatings have been created using a

The Ciência & Engenharia - Science & Engineering Journal
ISSN: 0103-944X
Volume 11 Issue 1, 2023
pp: 122 - 131

variety of methods, including physical vapour deposition (PVD) and arc ion plating [4]; each approach has advantages depending on the application. [5]

However, the deposition method used to coat the substrate with ZrN has an indirect impact on the performance of the thin coating created by the PVD procedure. [6]. In material science, it is widely acknowledged that the process will decide the structure before having an impact on the properties. [7] In order for the deposition process to fully satisfy the desired coating characteristic, the deposition process factors must be carefully chosen. The leftover stresses created in thin, hard coatings during cooling down after PDV coating are among the elements affecting coating quality. [8] The produced residual stresses must be carefully taken into account because they have a big impact on the coating qualities. The thin covering created by PVD contained a variety of flaws, including cracks, delamination, spallation, and buckling. The residual tension created in the coating directly correlates with crack defects.

Due to their superior qualities, including high hardness, mechanical strength, chemical inertness, and excellent high temperature stability, transitional metal (TM) nitride coatings have been thoroughly studied [9]. Zirconium nitride (ZrN) coatings have been used extensively on cutting tools, forming dies, bearings, and other objects among them [10–11]. The addition of the third element to the ZrN coating, ZrAlN coatings, which show greater hardness, lower friction coefficient, and excellent wear resistance, has been extensively studied to further improve its mechanical properties and high temperature stability [12–13].

Electron beam physical vapour deposition free electrons in a vacuum can be shaped into a narrow beam by the use of electric and magnetic fields. Electrons are transformed into heater kinetic energy where the stream collides with solid-state matter. The ability to accurately control this energy concentration in a small volume of matter has many benefits. An electron beam is a superb tool for heating applications, like welding, because the rapid temperature rise can even cause evaporation under severe working conditions. In addition to many other uses, electron beam technology is used in microelectronics for the electron-beam curing of colour printing, cable isolation treatment, electron lithography of sub-micrometer and nano-dimensional images, liquid crystal film manufacturing, and many other fields.

To enable electrons from the electron gun to reach the evaporation material, which can take the form of an ingot or rod, the deposition chamber in an EBPVD system must be evacuated to a pressure of at least 7.5105 Torr (102 Pa) [14]. In contrast, some contemporary EBPVD systems make use of an arc-suppression device and can function at vacuum pressures as low as 5.0103 Torr, for applications like use in tandem with magnetron sputtering [15]. A single EBPVD device can use a variety of evaporation materials and electron guns, each with a power range of tens to hundreds of kilowatts. Thermionic emission, field electron emission, and the anodic arc technique can all be used to produce electron beams. The produced electron beam is accelerated to have a high kinetic energy before being pointed at the substance that is evaporating. The electrons quickly lose energy when individuals contact the evaporation material [16].

The Ciência & Engenharia - Science & Engineering Journal
ISSN: 0103-944X
Volume 11 Issue 1, 2023
pp: 122 - 131

Through interactions with the evaporation substance, the electrons' kinetic energy is transformed into other types of energy. The substance used for evaporation is heated by the thermal energy created, which causes it to melt or sublimate. When the temperature and pressure are high enough, the melt or solid will turn into vapour. The mist that is produced afterward can be used to coat surfaces. The range of accelerating energies is 3 to 40 kV. 85% of the electron's kinetic energy can be transformed into thermal energy when the accelerating voltage is 20–25 kV and the beam current is a few amperes. Through the creation of X-rays and secondary electron emission, some of the incident electron energy is wasted.

Electromagnetic alignment, electromagnetic focusing, and the pendant drop configuration are the 3 major EBPVD configurations. While the pendant drop configuration uses a rod, electromagnetic alignment and electromagnetic focusing use evaporation material that is in the shape of an ingot. A rod will be fixed with one end in a socket and the other end in a copper crucible or hearth, which contains the ingots [17]. The socket and crucible must both be chilled. Water circulation is usually used to achieve this. When it comes to ingots, molten liquid may develop on its surface and can be maintained at a constant temperature by vertically shifting the ingot. The rate of vaporisation could be in the range of 102 g/(cm2•s).

2. Experimental procedure

Utilizing zirconium and CP aluminium, Al-Zr-N alloys with Zr contents varying from 3 to 10 wt% were created. The Al-Zr-N alloys were produced in an Ar environment in a vacuum arc-melting furnace (SVT, Korea). The Al-Zr-N metal was homogenised at 1000 °C for 24 hours in an Ar atmosphere before being cooled in water at 0 °C. The Al-Zr-N metal ingots were produced as rods, each measuring 60 mm in length and 10 mm in diameter.

The HA coating layers were formed by electron beam physical vapor deposition (EB-PVD) method on the Al–Zr-N alloy. The deposition target material of HA used in the experiment was synthesized by human tooth ash. The powder was compressed into pellets and thereafter subjected to a heat treatment that causes the powder particles to fuse together by means of solid-state diffusion. The HA pellet was sintered in air at 1200 °C for 2 h. The obtained HA target had a Ca/P ratio with around 1.67. For the e-beam deposition, an e-beam evaporator (TT-6, telemark, USA) were employed. After the chamber was evacuated to 5.0×10^{-3} torr by means of a mechanical rotary pump, a high vacuum of 2.0×10^{-7} torr was attained using a cryo pump.

The substrate was cleaned by sputtering using an Ar ion beam for 10 min. An e-beam was generated at a voltage of 7 kV to heat the evaporated. At the early stage of heating, the e-beam current was fixed to within 30 mA for degassing the evaporated. After stabilization, the current was increased to 50 mA and the vapor flux was generated for HA deposition on the rotating substrate to a thickness of 150 nm at a rate of 1 Å/s. Since the asdeposited coatings were amorphous, the coated substrates were then heat treated in Ar gas atmosphere for 1 h at 300 and 500 °C.

The Ciência & Engenharia - Science & Engineering Journal
ISSN: 0103-944X
Volume 11 Issue 1, 2023
pp: 122 - 131

The mechanical properties of the Al–Zr-N alloys were investigated by Vickers hardness tester (DM-20, AFFRI, Italy) and nano-indentation tester (TTX-NHT, Switzerland). Hardness of Al– Zr–N alloy was measured with a load (500 gf) applied for 10 s at the five regions of each alloy. Elastic modulus of Al–Zr-N alloy was obtained from a nano-indentation test with a 100 mN max load at an approach speed of 1500 nm/min.

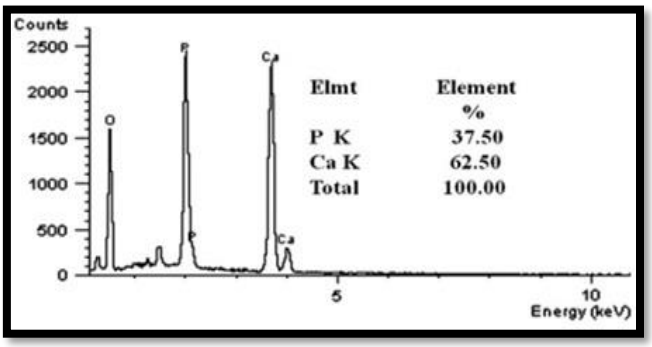

Fig.1 *EDX peaks of hydroxyapatite source target manufactured from human tooth ash*

The mechanical characteristics of the coatings deposited on E19 substrates were measured using the nanoindentation technique. The characteristic and reduced modulus were measured at a depth where they were not affected by the substrate. A coating cracking test was performed using an indenter in the form of an Ø50-μm diamond ball under loads of 100–1500 mN in steps of 100 mN. The speed of indenter sliding along the coating was 1 μms−1, while the indenter pass length (scratch) was 100 μm.

The mechanical behaviours of Al-Zr–N and multilayer [Al-Zr] N on E19 were investigated with a high-speed reciprocating friction and wear tester (MFT-R4000), at 25 °C and relative humidity of 33% under dry sliding conditions; a E19 steel ball (diameter: 6 mm) was used as the mating material. All tests were carried out at a sliding velocity of 40 mm/s and applied load of 3 N. After the test, the total volume of wear scar was calculated by at least three measurements using a surface three-dimensional profiler, and then the specific wear rate was determined as the volume of removed material at unit load over unit sliding distance.

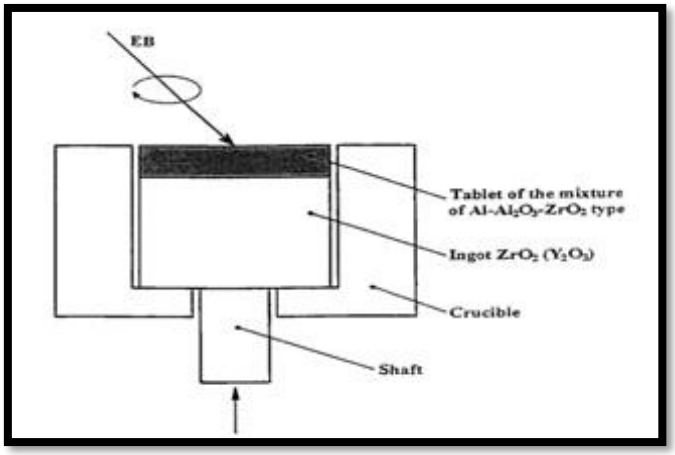

Fig.2 *Schematic of the device for GTBC production*

The Ciência & Engenharia - Science & Engineering Journal
ISSN: 0103-944X
Volume 11 Issue 1, 2023
pp: 122 - 131

In our experiments, the bond coat deposition was accomplished with a one-stage process. Flat stationary E19 steel alloy substrates measuring 35=10=44 mm thick were inserted to the vacuum chamber and preheated by the electron beam to a substrate temperature, T , of approx. 10508C. After s substrate heating the bond coat of a thickness of approx. 50 mm was deposited by Al-Zr-N ingot evaporation from a separate source. With essentially no process interruption, the tablet first and then the ceramic ingot after its finishing were deposited from the second individual source, producing the transition gradient zone Z. TGZ and TBC with a total thickness of approx. 140 mm. The 'source-substrate' separation was 350 mm.

An arc plasma source with the Zr0.5Al0.5 cathode and pulsed arc plasma source with a graphite cathode were used to deposit the Al-Zr–N coatings and Al-Zr-N layers in the multilayer coatings. The arc current was 55 A, while the pulse frequency was 3 Hz. The a-C layers were deposited using the pulsed arc plasma source only with the graphite cathode. The arc plasma source with the Cr0.5Al0.5 target and hollow plasma cathode were used for the depositions of the Al-Zr–N coatings and Al–Zr layers in the multilayer coatings. Decomposition of acetylene in an argon–acetylene mixture (30% Ar, 70% C2H2, P = 0.2 Pa) was performed in a non-selfsustained hollow-cathode pulsed-direct-current-(DC) discharge (U = 300 V, I = 3A). These conditions were used to deposit the a-C:H layers in the [Cr–Al–C(H)/a-C:H] n multilayer coatings.

The times of deposition of the separate layers in the multilayer coatings have been set so that the layer thickness does not exceed 50 nm. The time for each type of layer was calculated using a preliminary measured deposition rate of a single layer under the same conditions. The pair-of-layers numbers in the multilayer coatings were 20.The coating thickness was measured using a scanning electron microscopy (SEM) image of the cross section of the coating–substrate. The Zr, Al, and N contents in the coatings were determined by energy-dispersive X-ray spectroscopy using a QUANTA 200 microscope equipped with an EDAX analyser. The hydrogen in Al–Zr-N was detected by infrared spectroscopy (data not presented). The amounts of hydrogen in the films were not determined. micro hardness VHN measurements (L ==100 g) at the following location distances from the origin of bond coat TGZ contact area: level**1: 15]20 mm, level ** 2: 60]70 mm, level ** 3: 100]120 mm.

3. Results and discussion

The nano-hardness and young's modulus of the coatings are presented in Figure. The nano-hardness of the Al-Zr-N multilayers increases with decreasing modulation period L. This is in agreement with previous studies, e.g., for Ls7.5 nm the hardness of AlN/ZrN films achieves 40 GPa [18]. This hardening effect with decreasing L can be due to both grain size refinement discussed earlier and the high number of layer interfaces (dislocation blocking and strain effects) [19]. Young's modulus of the multi-layered coatings was found to range between the value for AlN (286 GPa) and the value for ZrN (349 GPa). It was found that the young's modulus decreases with decreasing modulation period L.

The Ciência & Engenharia - Science & Engineering Journal
ISSN: 0103-944X
Volume 11 Issue 1, 2023
pp: 122 - 131

The mechanism of hardness enhancement is explained by blocking interlaminar layers and dislocation at the interfaces and within the layers. This, in turn, is a result of differences in the shear modulus of the constituents, coherency strain present for small periodicity multilayer.

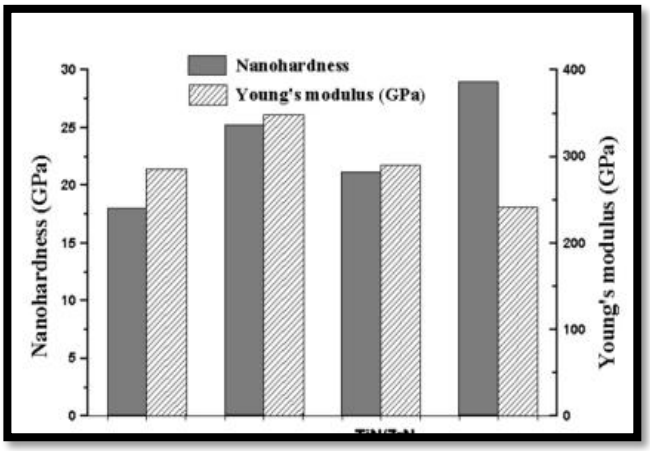

Fig. 3 *Nano-hardness and young's modulus of the Al-Zr-N multilayers*

with a significant lattice mismatch between the layers, the presence of grain boundaries and defects within the layers.

Another possible mechanism for hardness enhancement in nano-meter scale multilayers can be explained using the Koehler's model [20]. It is suggested that strength enhancement should be achieved in epitaxial heterostructures consisting of a few nano-meter thin layers of two metals A and B, with a high and low shear elastic modulus, respectively. The dislocations will be formed only in metal B having the lower shear modulus. Upon applied stress they will be hindered to cross the By/A interface, due to the repelling force of their image in A. The Koehler's prediction has been verified experimentally on different systems studied in the literature.

The nano-hardness of the (Al, Zr) N coatings as a function of the applied bias voltage is shown figure. The (Al, Zr) N coatings show significantly higher nanohardness values compared with that of binary coatings deposited under equivalent conditions, which may be ascribed to a solid-solution strengthening mechanism. The nano-hardness of pure AlN and ZrN films and 25.3 GPa, respectively, while the hardness of (Al, Zr)N films is approaching 40 GPa, close to the hardness of the B C carbide boron compound [21]. So, PVD technology, in which films are made with alternate and simultaneous cathode-ion bombardment of plasma stream of Aland Zr, in N gas atmosphere, allows getting to the class of super-hard materials.

The Ciência & Engenharia - Science & Engineering Journal
ISSN: 0103-944X
Volume 11 Issue 1, 2023
pp: 122 - 131

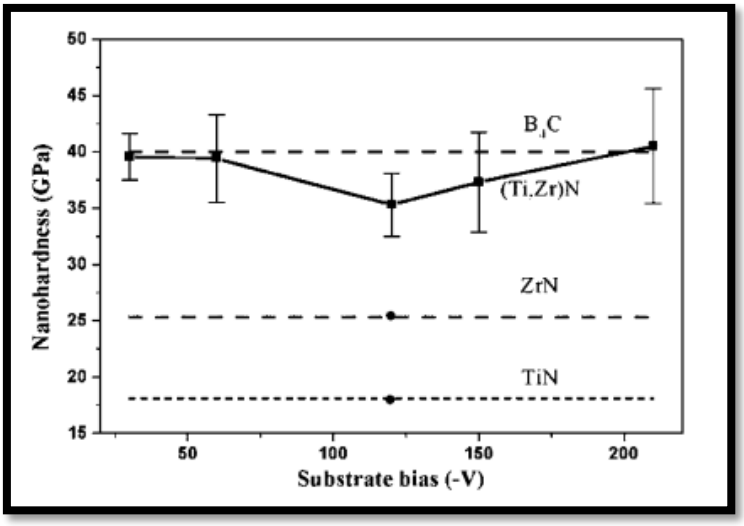

Fig. 3 *Nano-hardness and Substrate bias of the Ti-Zr-N multilayers*

The hardness of Al–Zr-N reaches 12.5 GPa, while that of Al-Zr-N is 8.9 GPa. The difference in hardness is associated with the coating structural features. The 5–20 nm nano of chromium carbide and nanocrystalline graphite increased the hardness of Al-Zr-N. Large amount of aluminium and the sp2 -bonded carbon clusters, owing to the hydrogen in the Al-Zr-N coating, reduced its hardness.

A friction coefficient of the Al-Zr-N is higher of a friction coefficient of Al-Zr-N. The Zr2AlN phase in Zr–Al–N(H) has a layer structure that serves as a solid lubricant, decreasing a friction coefficient. The roughness and friction coefficients of the multilayer coatings are lower as the upper layer in the multilayer is DLC (a-N:H) having a smooth surface[22].

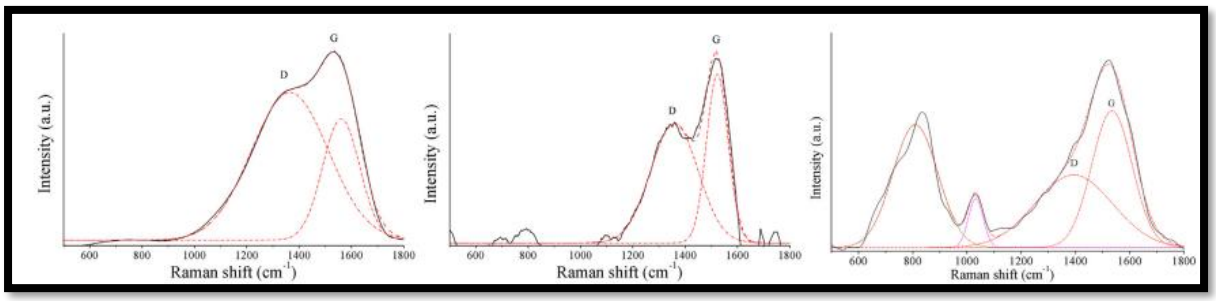

Fig. 4 *Roughness and friction coefficients of the multilayer coatings*

Regardless of the deposition technique, the hardness of the multilayer [Al-Zr-N]20 and [Al–Zr-N]20 coatings are close to those of the corresponding single Cr–Al–C and Cr–Al–C(H) coatings. However, their hardness are considerably lower than those of the a-C and a-C:H coatings. The hardness of a-N and a-N:H measured using the nanoindentation technique are larger than 25 GPa [22]. This could be attributed to the decreases in the hardness of the a-C or a-C:H layers due to their graphitisation under the bombardment by Zr+ and Al+ ions during the deposition of the Al-Zr-N layer. Although the hardness of the multilayer coatings are not increased, they are more crack- resistant compared with the single coating. Interface

The Ciência & Engenharia - Science & Engineering Journal
ISSN: 0103-944X
Volume 11 Issue 1, 2023
pp: 122 - 131

boundaries in these coatings deflect or reduce crack propagations and stress concentration, decreasing the critical load of crack appearance more than 1.6–2.0 times.

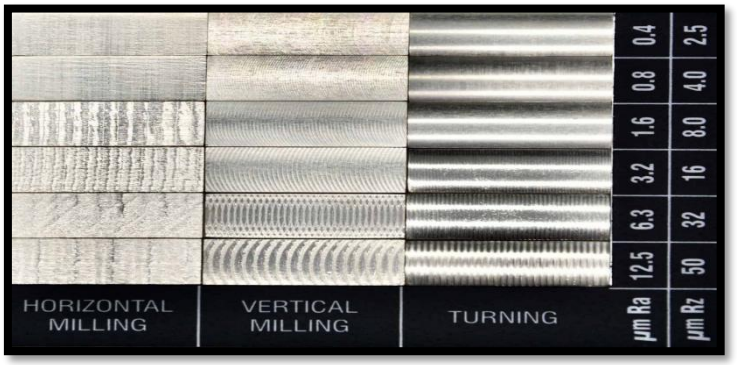

Fig. 5 *Hardness of the a-C or a-C:H layers due to their graphitisation*

The strengthened boundaries formed through the mixing of layers in [Cr–Al–C(H)/a-C:H]20 are indirectly confirmed by the Raman spectroscopy. The Raman spectra of a-C:H (upper layer in [Cr–Al–C(H)/aC:H]20), Cr–Al–C(H) coating, and [Cr–Al–C(H)/a-C:H]20 after the micro hardness test are presented in Figure. The spectrum of [Al-Zr-N]20 after the micro hardness test significantly differs from those of Al-Zr-N band in the range of 1200–1700 cm−1 without visible separation of the D and G modes is characteristic of DLC with a high sp3 content.

The bands in the range of 600–1100 cm−1 are most likely associated with the formation of Me–C bonds . Thus, the wear resistance of the multilayer coating is mainly associated with the layer structure, low friction coefficient, the interlayer boundaries and their strength.

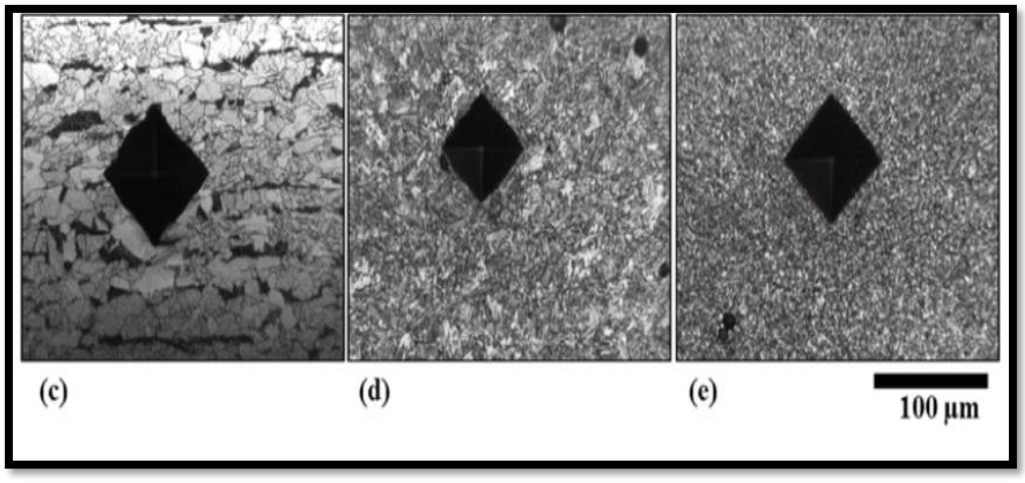

Fig. *6* Micro hardness test of Al-Zr-N band in the range of 1200–1700 cm^{-1}

Conclusion

To examine the structures of Zr-Al-N, pin on disc, micro hardness, and micro abrasion were used. Clusters of nanocrystalline graphite were found in Zr-Al-N along with the amorphous

The Ciência & Engenharia - Science & Engineering Journal
ISSN: 0103-944X
Volume 11 Issue 1, 2023
pp: 122 - 131

matrix, zirconium nitrate, and a small bit of nanograins. These clusters of graphite were present as spherical inclusions and plates and probable contained multiple graphene layers. The high hardness and corrosion resistance were given by this structure. Properties of multilayer coatings are influenced synergistically by the structures and mechanical traits of individual layers as well as the strength and structure of interlayer borders.

Future development trends will emphasise the inclusion of new components in coverings. electric current In order to combine the benefits of two coatings, a nano coating was prepared on the surface of the substrate using physical vapour deposition technology, and organic substance was then deposited on the nano coating. Devices with PVD coatings have increased toughness, wear resistance, and corrosion resistance.

References

[1] E. Santner, D. Klaffke, and G. Meier zu Köcker, "Comprehensive tribological characterization of thin TiN-based coatings," Wear, vol. 190, no. 2, pp. 204–211, 1995.

[2] W. J. Chou, G. P. Yu, and J. H. Huang, "Mechanical properties of TiN thin film coatings on 304 stainless steel substrates," Surf. Coatings Technol., vol. 149, no. 1, pp. 7–13, 2002.

[3] B. Škorić, D. Kakaš, M. Rakita, N. Bibić, and D. Peruškob, "Structure, hardness and adhesion of thin coatings deposited by PVD, IBAD on nitrided steels," Vacuum, vol. 76, no. 2–3, pp. 169–172, 2004

[4] G. Li, L. Zhang, F. Cai, Y. Yang, Q. Wang, and S. Zhang, "Characterization and corrosion behaviors of TiN/TiAlN multilayer coatings by ion source enhanced hybrid arc ion plating," Surf. Coatings Technol., vol. 366, no. February, pp. 355–365, 2019.

[5] B. Navinšek, P. Panjan, and I. Milošev, "PVD coatings as an environmentally clean alternative to electroplating and electroless processes," Surf. Coatings Technol., vol. 116– 119, pp. 476–487, 1999.

[6] J. Mao, M. Liu, Z. Deng, K. Wen, C. Deng, K. Yang, Z. Chen "Coating deposition regularity depended on orientation difference in PS-PVD plasma jet," Chinese J. Aeronaut., no. February, 2020. DOI: https://doi.org/10.1016/j.cja.2019.11.017.

[7] A. Baptista, F. J. G. Silva, J. Porteiro, J. L. Míguez, G. Pinto, and L. Fernandes, "On the Physical Vapour Deposition (PVD): Evolution of Magnetron Sputtering Processes for Industrial Applications," Procedia Manuf., vol. 17, pp. 746–757, 2018.

[8] V. Teixeira, "Residual stress and cracking in thin PVD coatings," Vacuum, vol. 64, no. 3–4, pp. 393–399, 2002.

[9] KIM K H. Hybrid functional multi-component composite films for hard coating applications [J]. Journal of Ceramic Processing Research, 2009, 10: 1−9.

[10] KAWANA A, ICHIMURA H, IWATA Y, ONO S. Development of PVD ceramic coatings for valve seats [J]. Surface and Coating Technology, 1996, 86−87(1−3): 212−217.

[11] MAKABE R, NAKJIMA S, TABATA O. Dependence of the hardness of titanium nitride prepared by plasma chemical vapour deposition on the gas flow rate and the r.f. power [J]. Thin Solid Films, 1986, 137(1): 49−50.

[12] SUSZKO T, GULBIŃSKI W, JAGIELSKI J. The role of surface oxidation in friction processes on molybdenum nitride thin films [J]. Surface and Coating Technology, 2005, 194(2−3): 319−324.

[13] RUDNIK P J, GRAHAM M E, SPROUL W D. High rate reactive sputtering of MoNx coatings [J]. Surface and Coating Technology, 1991, 49(1−3): 293−297

[14] Harsha, K. S. S, "Principles of Physical Vapor Deposition of Thin Films", Elsevier, Great Britain (2006), p. 400.

[15]http://telemark.com/electron_beam_sources/arc_suppression.php?cat=1&id=Arc+Suppression+Sources Archived 2012-12-12 at the Wayback Machine.

[16] George, J., "Preparation of thin films", Marcel Dekker, Inc., New York (1992), p. 13–19.

[17] Madou, M. J., "Fundamentals of Microfabrication: The science of Miniaturization" 2nd Ed., CRC Press (2002), p. 135–6.

[18] X.T. Zeng, S. Zhang, S.Q. Sun, Y.C. Liu, Thin Solid Films 424 (2003) 99–102.

[19] X. Chu, S.A. Branett, J. Appl. Phys. 77 (9) (1995) 4403.

[20] J.S. Koehler, Phys. Rev. B 2 (1970) 547.

[21] A.R. Andrievsky, I.I. Spivak. Prochnost' tugoplavkikh soedinenii i materialov na ikh osnove, Sprav. Izdanie, Chelabinsk, Mettalurgia, 1989, p. 368.

[22] N.V. Gavrilov, A.S. Mamaev, S.A. Plotnikov, A.P. Rubshtein, I.Sh. Trakhtenberg, V.A. Ugov, Comparison testing of diamond-like a-C:H coatings prepared in plasma cathode-based gas discharge and ta-C coatings deposited by vacuum arc, Surf. Coat. Technol. 204 (24) (2010) 4018–4024.

[23] Hariharan.R, Raja.R, Golden Renjith Nimal R J, Structural Tribological Characterization and Mechanical Properties of Ti-Zr-N Coating Deposited By RF/DC Magnetron Sputtering, J. Mech. Cont.& Math. Sci., Special Issue, No.-2, August (2019) pp 744-754.